AIP Journal of Applied Physics

A percolative approach to investigate electromigration failure in printed Ag structures

Zhao Zhao, Avinash Mamidanna, Christopher Lefky, Owen Hildreth, and T. L. Alford

Citation: Journal of Applied Physics **120**, 125104 (2016); doi: 10.1063/1.4963755
View online: http://dx.doi.org/10.1063/1.4963755
View Table of Contents: http://scitation.aip.org/content/aip/journal/jap/120/12?ver=pdfcov
Published by the AIP Publishing

A percolative approach to investigate electromigration failure in printed Ag structures

Zhao Zhao, Avinash Mamidanna, Christopher Lefky, Owen Hildreth, and T. L. Alford[a)]
School for Engineering Matter, Transport, and Energy, Arizona State University, PO Box 876016, Tempe, Arizona 85287, USA

(Received 3 August 2016; accepted 15 September 2016; published online 29 September 2016)

The ease of fabrication and wide application of printed microelectronics are driving advances in reactive inks. The long-term performance of structures printed using reactive ink is important for their application in microelectronics. In this study, silver lines are printed with low-temperature, self-reducing, silver-diamine based ink. The electromigration failure of the printed silver is first studied using Black's equation. However, due to the porous nature of the printed Ag line, Black's equation is not the best fit for predicting the lifetime, this is because Black's equation does not take into account morphology-induced current crowding. We find that the resistivity of the printed Ag lines can be described (as a function of void fraction) by percolation theory. In addition, we also demonstrate that the failure lifetimes of the printed Ag can be predicted quite well by a percolative model of failure. *Published by AIP Publishing*. [http://dx.doi.org/10.1063/1.4963755]

I. INTRODUCTION

Printed microelectronics have the potential for broad application and ease of use. This has been a driving force for significant advances in the inks that are used to print conducting lines. Such advances include lower sintering temperatures and lower resistances.[1–4] For example, newer nanoparticle-based silver inks can be chemically sintered at room temperature using polyanionic compounds.[5,6] Despite these advances, very few industries outside of the photovoltaic industry have adopted silver inks for their metallization schemes and even fewer use drop-on-demand (DOD) printed inks in real-world applications. This limited adoption of DOD printed electronics can be attributed to the limited availability of commercial-scale DOD printers capable of handling large production volumes with high resolutions and the high cost of DOD-compatible nanoparticle inks. Reactive inks are a new approach to DOD printed electronics that are easy to synthesize and that often do not require high-temperature sintering.[7,8] Unlike traditional inks that print clusters of particles, reactive inks print chemical precursors that react to form a solid material.[9,10] These reactions can be initiated by elevated substrate temperatures (thermally), solvent or stabilizing agent evaporation (chemically), or by some increased catalytic activity of the substrate (kinetically).[9,11–17] Recent advances in silver,[9] copper,[10] and aluminum[13,18] reactive inks have brought the reaction temperatures of these inks to below 180 °C and to even room temperature for silver-diamine based inks.[7,19,20] Compared to silver paste and nanoparticle-based inks, these new reactive inks provide superior conductivities (that are close to bulk material values) at lower temperatures and significantly lower costs. Applications for reactive inks include printed electronics,[9] stretchable electronics,[8] photovoltaic metallization,[21] and more.

The long-term performance of conducting lines that are printed with reactive Ag inks is currently unknown. This is because the most promising, low-temperature reactive ink chemistries for Ag, Cu, and Al are fairly new, with keystone publications having appeared only within the last few years.[9,10,13,20,22] As a result, the relationships among processing parameters, printed physical structure, material properties, and long-term performance have yet to be studied in detail. Of particular concern is how the porous nature of silver that is printed from a reactive silver ink impacts its properties and reliability. Electromigration and Joule heating are two phenomena that contribute to early failure in electronic devices. For a high-quality, solid material, electromigration (EM) generates voids that, due to current crowding, lead to localized Joule heating and rapid device failure.[23] The failure time of metal lines due to electromigration is typically predicted by Black's equation, which correlates the lifetime with the current density and temperature during the electromigration.[24] Since reactive inks currently print porous materials with a large volume-fraction of voids,[7] these materials should experience earlier failure than conducting elements fabricated using traditional methods (DC sputter coating, evaporation, electrochemical deposition, etc.). However, no studies have been published that detail the performance reliability of these printed reactive inks under a bias (temperature or current). Initial stress tests of printed silver reactive inks showed lifetimes that were quite random and that were independent of the current density. A deeper understanding of the relationship between morphology and failure mechanisms is needed before reactive silver inks (RSI) can replace more established particle-based inks and pastes.

In this work, we have studied the failure mechanisms of silver lines that were printed using a low-temperature, self-reducing, silver-diamine based ink. These studies demonstrated that Black's equation does not suitably account for morphology-induced current crowding when predicting the lifetimes of printed silver or other porous conducting elements. Overall, a model is needed that can take into account the effects of physical structure, mass-transport, and other

[a)]E-mail: TA@asu.edu. Tel.: 001 480 965 7471.

degradation mechanisms that can impact the lifetimes of porous or "imperfect" printed electronic devices. In this work, we demonstrate that a percolation-based model (for predicting the electromigration failure time) is suitable for predicting the increase in resistance of porous conducting lines under a current bias.

II. EXPERIMENTAL

The base silver ink (that was used for this study) was prepared following Lewis' reactive silver ink recipe.[9] All of the chemicals were used as received: silver acetate ($C_2H_3AgO_2$, anhydrous 99%, Alfa Aesar); ammonium hydroxide (NH_4OH, 28–30 wt. %, ACS grade, BDH Chemicals); formic acid (CH_2O_2, ≥96%, ACS reagent grade, Sigma Aldrich); and ethanol (EtOH, C_2H_6O, 99.5 wt. %, Koptec). 1.0 g of silver acetate was dissolved in 2.5 ml ammonium hydroxide. The solution was then stirred for 2 min on a vortex mixer to dissolve the silver acetate. Next, 0.2 ml of formic acid was added in two steps with a quick stir at the end of each step. The ink was then allowed to sit for 12 h in the dark at room temperature before being filtered through a 450 nm nylon filter. Following this, the ink was stored at 4 °C (refrigerator temperature) until it was used.

A mixture of 0.5 M tin (II) chloride solution in deionized water mixed 1:1 by volume with 0.5 M HCl was used as a sensitizing adhesion promoter[14] to keep the silver samples from peeling off from the glass substrate. The substrates were dipped in this solution for 300 s and dried using N_2. Silver reactive ink lines and contact pads were printed using a MicroFab Jetlab II micro-dispensing inkjet printer. Drop volume, velocity, and quality were observed using a horizontal camera and strobe light. The Jetlab II was equipped with an MJ-ATP-01 piezoelectric-driven printer head with a 60 μm orifice coated with a diamond-like coating to reduce wetting. The mean measured droplet size was 40 μm when printed with rise and echo driving voltages of ±25 V and dwell and echo times of 5 μs and 5 μs, respectively.

Single-line test structures were printed using 1:1 EtOH:Ag ink on the glass substrates, at 78 °C. Each of the printed lines had a length of 5 mm with a pitch of 25 μm between droplets and a measured droplet diameter of 100 μm. A Dektak XT stylus (12.5 μm stylus tip diameter) profilometer was used to collect cross-section profiles across each sample. The cross-section area of each sample was calculated by integrating the area under the measured profile.

The structures were then tested for reliability on a probe station (MC Systems, Inc., Model 8832) equipped with a temperature-controlled hot stage. The samples were tested at an elevated temperature of 94 °C to accelerate the failure process. Since early failure modes occurred at the interface between the probe and the contact pad instead of at the Ag line, conductive silver paint (Colloidal silver liquid, Ted Pella, Inc.) was applied on the contact pads in order to increase the contact surface area and to decrease the contact resistance between the probe and the contact pads to avoid the failure at their interface. The samples were tested using two probes in contact with opposite pads. A constant current was applied across the probes using an Agilent DC power supply (N5752A) and the voltage drop between the probes was measured every 1 s using a Keysight digital multimeter (34461A) until an open occurred in the line. Several different current values were applied to study the failures under different current stresses.

III. RESULTS AND DISCUSSION

Typically, the failure time of a metal line can be predicted by using Black's equation[24]

$$t_f = A_B J^{-n} \exp\left(-\frac{E_a}{k_B T}\right), \tag{1}$$

where A_B is a constant, J is the current density in A/cm^2, n is the current-density exponent, E_a is the activation energy in eV, k_B is Boltzmann's constant, and T is the substrate temperature in Kelvin. From Black's equation, n can be extracted by fixing the test temperature and varying the current density.[25,26]

The printed Ag line has a porous microstructure. A representative cross-section secondary electron microscopy (SEM) image of an as-printed Ag line is shown in Figure 1(a). The micrograph shows that the printed Ag film is porous and not solid. Due to the porous microstructure, only the Ag component (in the printed line) carries the current. As a result, the actual current-carrying cross-section area is equal to the cross-section area of Ag (A_{Ag}) if the pores are taken out from the printed Ag sample and the sample is 100% dense (0% porosity) as a result. A_{Ag} is calculated by dividing the volume of silver used in each printed Ag line by the line length. Each Ag line was printed using the same known amount of silver. Therefore, A_{Ag} is 152 μm^2, and it has the same value for all of the samples (the calculation of A_{Ag} is shown in the supplementary material). Next, the current density (J) is obtained by dividing the current (I) by A_{Ag} (to take into the account of current-carrying cross-section area). Six samples were tested using the same temperature but different current densities, until they failed. Their failure times (t_f) are plotted on a log-log scale, as the function of current density (J), as shown in Figure 1(b). For this study, the failure time is defined as the time that Ag line breaks. According to Eq. (1), t_f vs. J should be a linear function on the log-log plot and the current exponent n can be estimated by calculating the slope. However, it is evident from Figure 1(b) that the experimental results do not fall on a straight line as would be predicted by Black's equation.

We suspect that the erratic lifetimes of the RSI printed Ag lines is likely due to the porous microstructure of the lines, and that Black's equation cannot be used for these material systems because the equation assumes a solid cross-section for calculating the current density. This assumption breaks down for porous conductors because it does not account for current crowding in such porous materials.[27–29] With this in mind, it is clear that failure models that account for porosity and morphology must be used when working with porous printed conductors.

Percolation theory has been used to study the conductivity of carbon nanotube thin film networks.[30] Similarly, to

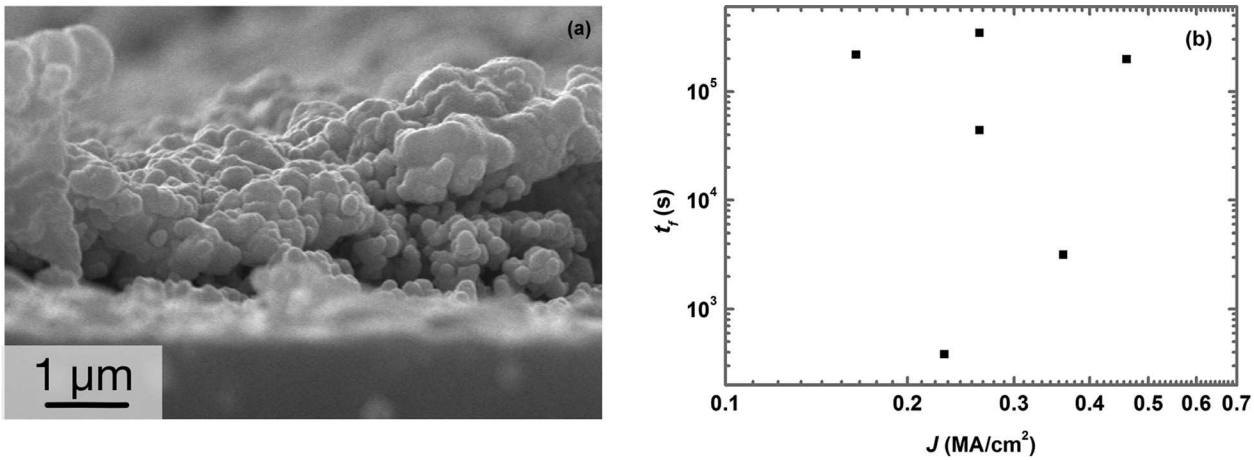

FIG. 1. (a) A cross-section SEM image of an as-imprinted Ag line; (b) Log t_f as a function of Log J in printed Ag samples. Note that the data do not lie on a straight line as would be predicted by Black's equation. This indicates that Black's equation cannot be applied to materials where the actual current density is not well known.

take into the account of the porosity of our printed sample, the conduction of this porous structure can be described by a standard (unbiased) percolation model.[31,32] The line can be viewed as a random network of insulators (voids) and conductive resistors (silver).[31,32] All of the resistors are assumed to have the same resistance, in order to simplify the model. Based on percolation theory, the resistivity (ρ) is a function of the void fraction, and is given by the following equation:[33]

$$\rho = \rho_0(1 - f_V)^{-m}, \tag{2}$$

where ρ_0 is the pre-factor and is proportional to the metal's bulk resistivity, and m is the percolation coefficient. The resistivity (ρ) of a printed Ag line is obtained from the measured resistance, the measured area, and the line length. f_V is the fraction of voids in the printed sample.

Our measurements show that the measured cross-section areas are different from sample-to-sample, even though the lines were printed using the same amount of Ag ink. This is an indication of the variation in porosity from sample-to-sample and even within the same sample. The porosity can be estimated by calculating the fraction of the voids in the sample (f_V)

$$f_V = 1 - \frac{V_{Ag}}{V_{measured}} = 1 - \frac{A_{Ag} \cdot l}{A_{measured} \cdot l} = 1 - \frac{A_{Ag}}{A_{measured}}, \tag{3}$$

where V_{Ag} and A_{Ag} are the volume and cross-section area if the printed Ag sample was 100% dense (0% porosity), $V_{measured}$ and $A_{measured}$ are the measured volume and measured cross-section area of the printed Ag sample as determined by profilometry, and l is the length of the printed Ag sample.

The ρ and f_V of several printed Ag samples were determined, to validate the percolation model on the printed Ag sample. The resulting ρ is plotted as a function of f_V and can be fitted by Eq. (2), as shown in Figure 2. The values of ρ_o and m were calculated to be 1.51×10^{-5} Ω cm, and 0.91, respectively. Using a least-squares model, the adjusted R-square of fit was 0.97. Based on this fit, we conclude that the conduction pathways of the printed reactive inks can be described by the standard percolation model.

Given that the conduction occurs via a percolation process, one would expect that the failure should also occur by such a process. When failure occurs by the standard percolative model, the damage would be uniform and dependent on a single test parameter.[31,32] In the case of electromigration, the failure occurs due to void formation and coalescence during the current stressing.[23] The percolative model for predicting the electromigration failure has to be biased given that the failure is nonhomogeneous, and it depends on the position and time.[31,32] Monte-Carlo simulations have been used to describe the evolution of resistance for biased percolation.[31,32] The scaling of the resistance as a function of time ($R(t)$) is given by

$$R(t) = \gamma R_0 \left(1 - \frac{t}{t_f}\right)^{-u}, \tag{4}$$

where R_0 is the initial resistance, γ is a statistical variation factor which does not have physical meaning but is due to

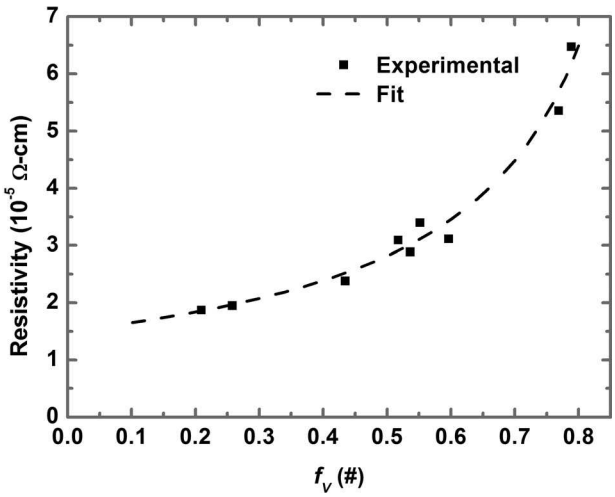

FIG. 2. ρ as a function of void fraction (f_V) from the printed Ag samples before EM testing. Experimental fit of $\rho = \rho_0(1 - f_V)^{-m}$ with $\rho_0 = 1.5 \times 10^{-5}$ Ω cm $m = 0.91$; the Adjusted R-square of fit was 0.97 using a least square fit method to fit lnR vs. $\ln(1 - f_V)$, in order to fit a linear line. These results show that the percolation model adequately models the conduction pathways for these materials.

statistical variation during data collection, t is time under bias, t_f is the failure time, and μ is the percolation parameter. μ is dependent on the current density and the temperature applied on the sample.[31,32]

Two printed samples were tested under current densities of 2.63 MA/cm^2 and 3.62 MA/cm^2. Both samples were tested at 94 °C until an open-circuit was measured (i.e., failure). Their resistance as a function of time is plotted in Figure 3. Given that their initial resistance and failure times are known, the γ and μ can be extracted by fitting the R vs. t curves using Eq. (4). A typical fit using Eq. (4) is shown in Figure 3. The extracted results and detailed parameters from the samples are listed in Table I. The results show that μ has the same value (of 0.012) when the samples have the same current density (of 2.63 MA/cm^2). However, μ had a value of 0.048 when the sample was tested under a different current (of 3.62 MA/cm^2). This result is consistent with the fact that μ depends on the current density and temperature in the percolation model. The deviation of R from the fitting model between 2000 and 2500 s is probably due to the evolution of the voids/pores in the printed Ag line. It has been proposed[34] that the resistance change depends on the void shape and the change in void volume, $\Delta R/R = f{\cdot}\Delta V/V$.[34] The volumes and shapes of the local pores/voids in the porous Ag line are more likely to change due to current-induced mass transportation. This will cause a deviation of the R from the model, since the model does not take into account the effects of changes in the local voids.

The percolative model can be further modified to incorporate the void fraction. In the percolative model, R_0, which is the initial resistance of the sample, can be related to the void fraction using Eq. (2). This can be expressed as

$$R_0 = \frac{\rho \cdot l}{A_{measured}} = \frac{\rho_0 (1 - f_V)^{1-m} \cdot l}{A_{Ag}}. \quad (5)$$

Hence, the void fraction can be incorporated into Eq. (4), by using Eq. (5)

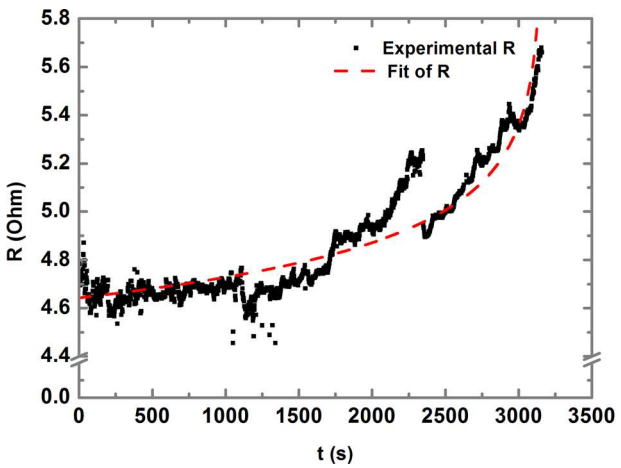

FIG. 3. Resistance of printed Ag sample as a function of time for a current density of 3.62 MA/cm^2.

TABLE I. The current density (J), void fraction (f_V), initial resistance (R_o), failure time (t_f), and parameters (γ and μ) extracted by fitting Eq. (4).

Sample ID	J (MA/cm^2)	f_V	R_o	t_f (s)	γ	μ
a	3.62	0.926	4.75	3159	0.97	0.048
b	2.63	0.960	4.13	43 994	0.96	0.012
c	2.63	0.955	5.00	342 536	0.93	0.012

$$R(t) = \gamma \cdot \frac{\rho_0 (1 - f_V)^{1-m} \cdot l}{A_{Ag}} \left(1 - \frac{t}{t_f}\right)^{-u}. \quad (6)$$

Inspection of Eq. (6) shows that the porosity has a direct impact on the time dependent resistance during biasing at high current levels. In addition, the EM failure-time and the reliability of printed lines can be predicted using percolation theory. Future work will focus on the use of Eq. (6) to experimentally demonstrate that for similar structures (i.e., similar metals and with similar porosity) that are undergoing EM degradation, the exponents m and μ can be accurately extracted from a small population of samples.

IV. CONCLUSION

Ag metallization structures were printed by using reactive Ag ink. The reliability of the printed single-line Ag structure was tested through EM. The test results were first analyzed using Black's equation. However, J vs. t did not follow Black's equation. SEM analysis showed that the printed Ag lines are porous. These results indicated that it is inappropriate to apply Black's equation to porous structures. In contrast, the conduction in the porous Ag line was successfully described by using percolation theory. Therefore, we expected that the percolative model should be able to describe the failures of the porous printed Ag lines. Our analysis shows that R vs. t can be fitted well by the percolative model. A dependence of μ on current density is observed in the experiment. This further supports the hypothesis that the percolative model is valid for describing failures of porous printed Ag lines. A model that links the physical structure and mass-transport to the lifetime is obtained by modifying the percolative model.

SUPPLEMENTARY MATERIAL

The supplementary material shows the detailed calculation for cross-section area of Ag (A_{Ag}) if the pores are moved from the printed Ag sample and the sample is 100% dense (0% porosity) as a result.

ACKNOWLEDGMENTS

The authors thank N. David Theodore in NXP Semiconductors N.V. for his great help in offering suggestion on preparing manuscript. This work was partially supported by the National Science Foundation (C. Ying, Grant No. DMR-0902277) to whom the authors are greatly indebted.

[1]A. Kamyshny, J. Steinke, and S. Magdassi, Open Appl. Phys. J. **4**, 19 (2011).
[2]J.-T. Wu, S. L.-C. Hsu, M.-H. Tsai, and W.-S. Hwang, J. Phys. Chem. C **115**, 10940 (2011).

[3]S. Magdassi, M. Grouchko, and A. Kamyshny, Materials **3**, 4626 (2010).
[4]B. Lee, Y. Kim, S. Yang, I. Jeong, and J. Moon, Curr. Appl. Phys. **9**, e157 (2009).
[5]S. Magdassi, M. Grouchko, O. Berezin, and A. Kamyshny, ACS Nano **4**, 1943 (2010).
[6]M. Grouchko, A. Kamyshny, C. F. Mihailescu, D. F. Anghel, and S. Magdassi, ACS Nano **5**, 3354 (2011).
[7]C. Lefky, A. Mamidanna, Y. Huang, and O. Hildreth, Phys. Status Solidi A, 1 (2016).
[8]A. Mamidanna, Z. Song, C. Lv, C. S. Lefky, H. Jiang, and O. J. Hildreth, ACS Appl. Mater. Interfaces **8**, 12594 (2016).
[9]S. B. Walker and J. A. Lewis, J. Am. Chem. Soc. **134**, 1419 (2012).
[10]Y. Rosen, M. Grouchko, and S. Magdassi, Adv. Mater. Interfaces **2**, 1400448 (2015).
[11]Y. Farraj, M. Grouchko, S. Magdassi, F. Koch, M. Wittkötter, M. Müller, I. Reinhold, and W. Zapka, "Ink-jet printed copper complex MOD ink for plastic electronics," in *International Conference on NIP & Digital Fabrication Conference* (Society for Imaging Science and Technology, 2014), p. 191.
[12]D.-H. Shin, S. Woo, H. Yem, M. Cha, S. Cho, M. Kang, S. Jeong, Y. Kim, K. Kang, and Y. Piao, ACS Appl. Mater. Interfaces **6**, 3312 (2014).
[13]H. M. Lee, J. Y. Seo, A. Jung, S.-Y. Choi, S. H. Ko, J. Jo, S. B. Park, and D. Park, ACS Appl. Mater. Interfaces **6**, 15480 (2014).
[14]H. M. Lee, H. B. Lee, D. S. Jung, J.-Y. Yun, S. H. Ko, and S. B. Park, Langmuir **28**, 13127 (2012).
[15]D. Li, D. Sutton, A. Burgess, D. Graham, and P. D. Calvert, J. Mater. Chem. **19**, 3719 (2009).
[16]D. S. Ginley, C. J. Curtis, A. Miedaner, M. F. A. M. Van Hest, and T. Kaydanova, U.S. No. Patent 8,641,931 (4 February 2014).
[17]J. J. Valeton, K. Hermans, C. W. Bastiaansen, D. J. Broer, J. Perelaer, U. S. Schubert, G. P. Crawford, and P. J. Smith, J. Mater. Chem. **20**, 543 (2010).
[18]H. M. Lee, S. Y. Choi, K. T. Kim, J. Y. Yun, D. S. Jung, S. B. Park, and J. Park, Adv. Mater. **23**, 5524 (2011).
[19]G. Jenkins, Y. Wang, Y. L. Xie, Q. Wu, W. Huang, L. Wang, and X. Yang, Microfluid. Nanofluid. **19**, 251 (2015).
[20]Y. Farraj, M. Grouchko, and S. Magdassi, Chem. Commun. **51**, 1587 (2015).
[21]A. Jeffries, A. Mamidanna, J. Clenney, L. Ding, O. Hildreth, and M. Bertoni, "Innovative methods for low-temperature contact formation for photovoltaics applications," in *IEEE 42nd Photovoltaic Specialists Conference (PVSC)* (IEEE, 2015), p. 1.
[22]Q. Huang, W. Shen, Q. Xu, R. Tan, and W. Song, Mater. Lett. **123**, 124 (2014).
[23]T. Alford, E. Misra, S. Bhagat, and J. Mayer, Thin Solid Films **517**, 1833 (2009).
[24]J. R. Black, IEEE Trans. Electron Devices **16**, 338 (1969).
[25]E. Misra, N. Theodore, J. Mayer, and T. L. Alford, Microelectron. Reliab. **46**, 2096 (2006).
[26]A. Indluru, E. Misra, and T. L. Alford, IEEE Electron Device Lett. **30**, 1134 (2009).
[27]E. C. Yeh, W. Choi, K. Tu, P. Elenius, and H. Balkan, Appl. Phys. Lett. **80**, 580 (2002).
[28]S. Gousseau, S. Moreau, D. Bouchu, A. Farcy, P. Montmitonnet, K. Inal, F. Bay, M. Zelsmann, E. Picard, and M. Salaun, Microelectron. Reliab. **55**, 1205 (2015).
[29]H. Ceric and M. Rovitto, in *Impact of Microstructure and Current Crowding on Electromigration: A TCAD Study* (IEEE, 2015), p. 194.
[30]X. Tian, M. L. Moser, A. Pekker, S. Sarkar, J. Ramirez, E. Bekyarova, M. E. Itkis, and R. C. Haddon, Nano Lett. **14**, 3930 (2014).
[31]C. Pennetta, L. Reggiani, and G. Trefán, Phys. Rev. Lett. **84**, 5006 (2000).
[32]E. Misra, M. M. Islam, M. Hasan, H. Kim, and T. L. Alford, Microelectron. Reliab. **45**, 391 (2005).
[33]S.-Y. Chang, C.-F. Chen, S.-J. Lin, and T. Z. Kattamis, Acta Mater. **51**, 6291 (2003).
[34]A. Scorzoni, I. De Munari, H. Stulens, and V. D'Haeger, J. Appl. Phys. **80**, 143 (1996).